

# Simple device for the direct visualization of oral-cavity tissue fluorescence

## Pierre M. Lane

British Columbia Cancer Research Center  
Cancer Imaging Department  
675 West 10th Avenue  
Vancouver, British Columbia V5Z 1L3  
Canada  
E-mail: plane@bccrc.ca

## Terence Gilhuly Peter Whitehead

LED Medical Diagnostics Inc.  
#201-15047 Marine Drive  
White Rock, British Columbia V4B 1C5  
Canada

## Haishan Zeng

British Columbia Cancer Research Center  
Cancer Imaging Department  
675 West 10th Avenue  
Vancouver, British Columbia V5Z 1L3  
Canada

## Catherine F. Poh

### Samson Ng

The University of British Columbia  
Faculty of Dentistry  
2199 Westbrook Mall  
Vancouver, British Columbia V6T 1Z4  
Canada

## P. Michele Williams

British Columbia Cancer Research Center  
Oral Oncology Department  
675 West 10th Avenue  
Vancouver, British Columbia V5Z 1L3  
Canada

## Lewei Zhang

The University of British Columbia  
2199 Westbrook Mall  
Vancouver, British Columbia V6T 1Z4  
Canada

## Miriam P. Rosin

British Columbia Cancer Research Center  
Cancer Control Research Program  
675 West 10th Avenue  
Vancouver, BC V5Z 1L3  
and  
Simon Fraser University  
8888 University Drive  
Burnaby, British Columbia V5A 1S6  
Canada

## Calum E. MacAulay

British Columbia Cancer Research Center  
Cancer Imaging Department  
675 West 10th Avenue  
Vancouver, British Columbia V5Z 1L3  
Canada

**Abstract.** Early identification of high-risk disease could greatly reduce both mortality and morbidity due to oral cancer. We describe a simple handheld device that facilitates the direct visualization of oral-cavity fluorescence for the detection of high-risk precancerous and early cancerous lesions. Blue excitation light (400 to 460 nm) is employed to excite green-red fluorescence from fluorophores in the oral tissues. Tissue fluorescence is viewed directly along an optical axis collinear with the axis of excitation to reduce inter- and intraoperator variability. This robust, field-of-view device enables the direct visualization of fluorescence in the context of surrounding normal tissue. Results from a pilot study of 44 patients are presented. Using histology as the gold standard, the device achieves a sensitivity of 98% and specificity of 100% when discriminating normal mucosa from severe dysplasia/carcinoma *in situ* (CIS) or invasive carcinoma. We envisage this device as a suitable adjunct for oral cancer screening, biopsy guidance, and margin delineation.  
© 2006 Society of Photo-Optical Instrumentation Engineers.  
[DOI: 10.1117/1.2193157]

**Keywords:** autofluorescence; fluorescence imaging; oral cancer; squamous cell carcinoma.

Paper 05230R received Aug. 12, 2005; revised manuscript received Nov. 13, 2005; accepted for publication Dec. 16, 2005; published online Apr. 10, 2006.

## 1 Introduction

Oral squamous cell carcinoma (SCC) is believed to progress from oral premalignant lesions (OPLs)—hyperplasia, increasing degree of dysplasia (mild, moderate, and severe) into carcinoma *in situ* (CIS), and finally to invasive SCC (from stages I to IV). This disease is a source of substantial morbidity and mortality with over 275,000 new cases and 127,000 deaths worldwide<sup>1</sup> in 2002. In the United States, it is estimated that there will be<sup>2</sup> 29,370 new cases of oral cancer and 7320 deaths in 2005. Cancer stage at the time of the diagnosis is directly related to the disease morbidity: early detection enables minimally invasive treatment procedures. It also is related to the disease mortality: 5-yr survival rate is 81% for early stages of oral SCC versus 30% for late-stage disease.<sup>2</sup> However the 5-yr survival rate has remained dismal with little improvement over the last 30 yr (<50%), mainly due to the fact that a significant proportion of these cancers are still diagnosed late<sup>3</sup> (stages III and IV).

Ironically OPLs and early SCC have known clinical presentations, mostly as leukoplakia (white patches) and sometimes as erythroplakia (red patches). These lesions are present in a site that is readily accessible for visual inspection, possibly as part of an annual dental visit. Additionally there are known high-risk populations (e.g., elderly heavy smokers) that should be examined regularly. The main limitation is that

Address all correspondence to Pierre M. Lane, British Columbia Cancer Research Center, Cancer Imaging Dept., 675 West 10th Ave., Vancouver, BC V5Z 1L3, Canada. Tel: (604) 675-8087; Fax: (604) 675-8099; E-mail: plane@bccrc.ca

differential diagnosis of OPLs from the much higher incidence of lesions resulting from nonspecific inflammation and irritation (that also appear as white or red patches) is challenging even for experienced specialists. Patients may be reluctant to submit to an invasive and sometimes painful biopsy when their dentists' confidences as to the nature of the lesions is low. Furthermore, there is increasing awareness that many OPLs and early SCC are clinically occult and not visible under white-light examination. Together, these difficulties can result in a failure to biopsy and hence a delay in the diagnosis, since the actual assignment of risk requires a biopsy to determine the presence and degree of dysplasia/invasion.<sup>4</sup> The development of adjunct tools to facilitate the noninvasive screening of high-risk oral lesions in real time has the potential to significantly improve our ability to reduce the dismal morbidity and mortality of oral cancer.

While white-light visualization can perceive only a fraction of the spectral characteristics that differentiate diseased tissue from its normal counterpart, optical methods, particularly those based on fluorescence imaging and spectroscopy, will likely improve our ability to detect tissue changes, such as OPLs and early cancer. Recent studies have shown great promise in the screening and diagnosis of precancers in the lung,<sup>5</sup> uterine cervix,<sup>6</sup> skin,<sup>7</sup> and oral cavity.<sup>4,8-14</sup>

In this paper, we present a simple field-of-view device for the direct visualization of tissue fluorescence in the oral cavity. Instrumentation for fluorescence imaging requires a light source, excitation and emission filters, and a means of detection. The fluorescence can be detected and visualized directly by a human observer, as intended by the device described in this paper, or recorded by a camera and visualized indirectly. Recently, fluorescence imaging studies for the early detection of oral malignancies have employed indirect visualization—either photographic film or a sensitive or intensified CCD camera. De Veld et al. provide a good review of *in vivo* autofluorescence spectroscopy and imaging for oral oncology.<sup>15</sup> The methods of excitation, emission, and detection employed in several recent studies are briefly summarized here.

Onizawa et al.<sup>16,17</sup> used a custom UV-flash photography system to record porphyrin-like fluorescence in the oral cavity. Fluorescence was excited by the 360-nm spectral peak of the flash lamp and fluorescence was recorded on photographic film using a 480-nm long-pass filter. Lesions were classified based on the intensity and color of the fluorescence recorded on the film. The authors reported<sup>16</sup> 91% sensitivity and 84% specificity for discriminating benign from malignant lesions (and 94% sensitivity and 96% specificity for discriminating SCC and dysplasia from benign lesions).

Other groups have used commercially available autofluorescence systems and sensitive or intensified CCD cameras to image oral-cavity fluorescence. Betz et al.<sup>9,18</sup> and Paczona et al.<sup>19</sup> used a Storz endoscopy system configured for white-light and autofluorescence imaging. In autofluorescence mode, illumination from a xenon arc lamp at 375 to 440-nm excited fluorescence, which was detected by a sensitive color CCD camera through a 515-nm long-pass filter. Video frame integration for as long as 2 s was required.<sup>9</sup> The authors report a similar loss of fluorescence intensity at neoplastic lesions. Kulapeditharom and Boonkitticharoen<sup>14</sup> used the Xillix laser-induced autofluorescence endoscopy (LIFE) system in their study of head and neck cancers. The LIFE system, designed

for fluorescence bronchoscopy,<sup>20</sup> employs excitation at 442 nm and dual image-intensified cameras for detection in the green (480 to 520 nm) and red (>630 nm) emission channels. Lesions were classified based on the green-to-red fluorescence ratio displayed as a pseudocolor image. The authors found LIFE to be an effective and reliable tool for detecting head and neck cancers and reported increased sensitivity and specificity compared to white-light imaging.

More recently, Svistun et al. proposed a system for the direct visualization of oral cavity fluorescence.<sup>21</sup> In their device, excitation light is provided by a handheld illuminator and tissue fluorescence is observed along an axis slightly inclined from the illumination axis using special glasses. In their study, tissue fluorescence of freshly resected oral tissue was observed visually and photographed at specific excitation wavelengths suggested by previous studies of fluorescence spectroscopy<sup>10</sup> and optimal visual perception.<sup>22</sup> Perceived tumor margins, as determined from the fluorescence images and not observed directly through the viewing glasses, were correlated with histopathology. The sensitivity and specificity were 91 and 86% for the discrimination of normal tissue from neoplasia at the best excitation wavelength. The sensitivity and specificity were 75 and 43% for the same task using white-light images.

In contrast, the device presented in this paper employs coaxial optical pathways for excitation and emission. By employing coaxial illumination and imaging we hope to reduce inter- and intraoperator variability. In addition, we also present results based on the direct visual impression of oral cavity fluorescence rather than the indirect visualization from an image recorded on photographic film or detected by a CCD camera.

In an earlier version of the direct visualization device presented in this paper, tissue fluorescence was shown to more accurately estimate the histological margins of basal cell carcinoma (BCC). In a study of patients with BCC, tumor margins were delineated under white light and then again using direct fluorescent visualization.<sup>7,23,24</sup> Fluorescence visualization more accurately estimated the histological margins of the BCC.

There is clearly a need for a simple cost-effective screening device for the early detection of oral premalignant lesions. In this paper, we describe such a device, which aids in the direct visualization of tissue fluorescence for the early identification of precancers in the oral cavity. The study objective was to test this real-time device for its ability to discriminate high-risk OPLs and invasive SCCs from normal oral mucosa.

## 2 Material and Methods

### 2.1 Device

The device for direct fluorescence visualization (direct FV), illustrated schematically in Fig. 1, consists of a bench-top light source coupled to a handheld unit for visualization. The light source (X-Cite 120, EXFO) used a 120-W metal-halide arc lamp with integral elliptical reflector optimized for near-UV/blue reflection. The power coupled into the light guide was adjustable in steps by rotating a variable-pinhole wheel. Light was coupled from the light source to the handheld unit by a 0.59—numerical aperture (NA), 3-mm-diam liquid light guide (Lumatec, Germany). The handheld unit projected ex-

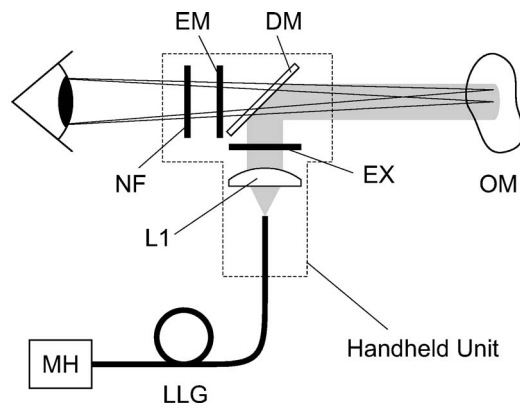


**Fig. 1** Schematic diagram of device for direct FV of oral mucosa: metal-halide light source (MH), liquid light guide (LLG), collimator lens (L1), excitation filter (EX), dichroic mirror (DM), oral mucosa (OM), emission filter (EM), and notch filter (NF).

citation light onto the oral mucosa and provided a viewing port coaxial with illumination for fluorescence visualization. A two-element lens system ( $f=25$  mm) collected light from the light guide and projected it onto the tissue through a low-fluorescence excitation filter (EX). Light exiting the lens system was nearly collimated. A dichroic mirror (DM) was employed to provide coaxial excitation and emission pathways. The emission filter (EM) passed the green-red fluorescent light and rejected the blue excitation light while the notch filter (NF) divided the fluorescent light spectrum into red and green components. Photographs of the light source and handheld unit are shown in Fig. 2.

The excitation and emission wavelengths were selected based on spectroscopic data and empirical measurements from previous unpublished studies. The excitation filter was a 60-nm bandpass filter centered at 425 nm (Chroma D425/60 $\times$ ) and provided an excitation spectrum composed primarily of the 405- and 436-nm peaks of the metal-halide lamp. The emission filter was a 475-nm long-pass (Schott GG475-3), while the center wavelength and bandwidth of the notch filter were chosen empirically to maximize the perceived color difference between normal and abnormal mu-

cosa. The upper end of the emission passband was determined by the sensitivity of the human visual system.

Photographs of tissue fluorescence were acquired for documentation only and were not used for the classification of lesions. Photographs were acquired using illumination from the direct FV system and a digital SLR (single lens reflex; Fuji FinePix S2 Pro) equipped with a long-pass filter (Schott GG475-3). The SLR was equipped with a 105-mm  $f/2.8$  macro lens (Nikkor Micro) and a ring flash (Nikon Macro Speedlight SB-29s) for white-light images.

## 2.2 Patients and Direct FV

Consenting patients with a history of biopsy-confirmed oral dysplasia or SCC were recruited from the Oral Health Study, an ongoing longitudinal study of oral leukoplakia at the British Columbia Cancer Agency (BCCA). The study was approved by the Institutional Review Board of the BCCA. These patients were referred primarily by community dentists to the Oral Dysplasia Clinic and the Head and Neck Oncology group at the BCCA for assessment and care.

Each follow-up visit for these patients involved an assessment, under white light, of the oral mucosa to identify new clinical lesions or alterations to previously identified clinical lesions. Particular attention was paid to sites of previous lesions (i.e., sites of prior oral SCC). After turning off the room light, the oral cavity was viewed with direct FV. The clinicians would then decide whether the oral lesions required biopsy based on standard clinical features (patient history, clinical appearance, and toluidine blue staining results<sup>25</sup>) and not based on the direct FV examination. For the biopsied lesions, histopathological reviews were conducted by oral pathologists in the Provincial Oral Biopsy Service at the Vancouver Hospital and Health Sciences Center (CP and LZ) and a histological diagnosis was assigned to each lesion. Since the objective here was to verify the effectiveness of the direct FV device in differentiating high-risk OPLs and invasive SCC from normal oral mucosa, we assessed the association with direct FV changes in the oral mucosa of biopsy-confirmed sites of normal and severe dysplasia, CIS, and invasive SCC. Fifty oral biopsies from 44 patients were included in this study.

## 3 Results

### 3.1 Device

The cone of blue excitation light emitted from the handheld unit produced a spot 44 mm in diameter on the tissue at a distance of 100 mm. At maximum power the peak irradiance at the tissue was 100 mW cm<sup>-2</sup>.

### 3.2 Direct FV and Pathology

Under direct FV, the normal oral mucosa emits various shades of pale green autofluorescence [Fig. 3(b)]. Clinical lesions that retained the normal green autofluorescence under direct FV were classified as lesions with FV retention (FVR). Tissue that showed a distinct reduction in the normal pale green and appeared as dark green to black was classified as FV loss (FVL) [Figs. 3(d) and 3(f)]. This assessment involved a comparison of the lesion site with both adjacent tissue and, as an anatomical control, with tissue on the contra lateral side.

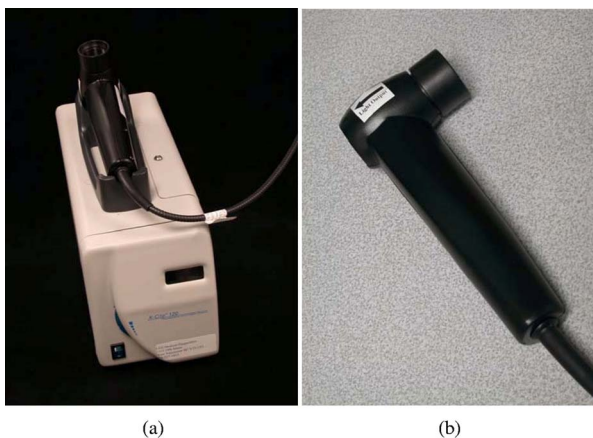


**Fig. 2** Direct FV instrumentation: (a) metal-halide light source with handheld unit in cradle and (b) handheld unit.

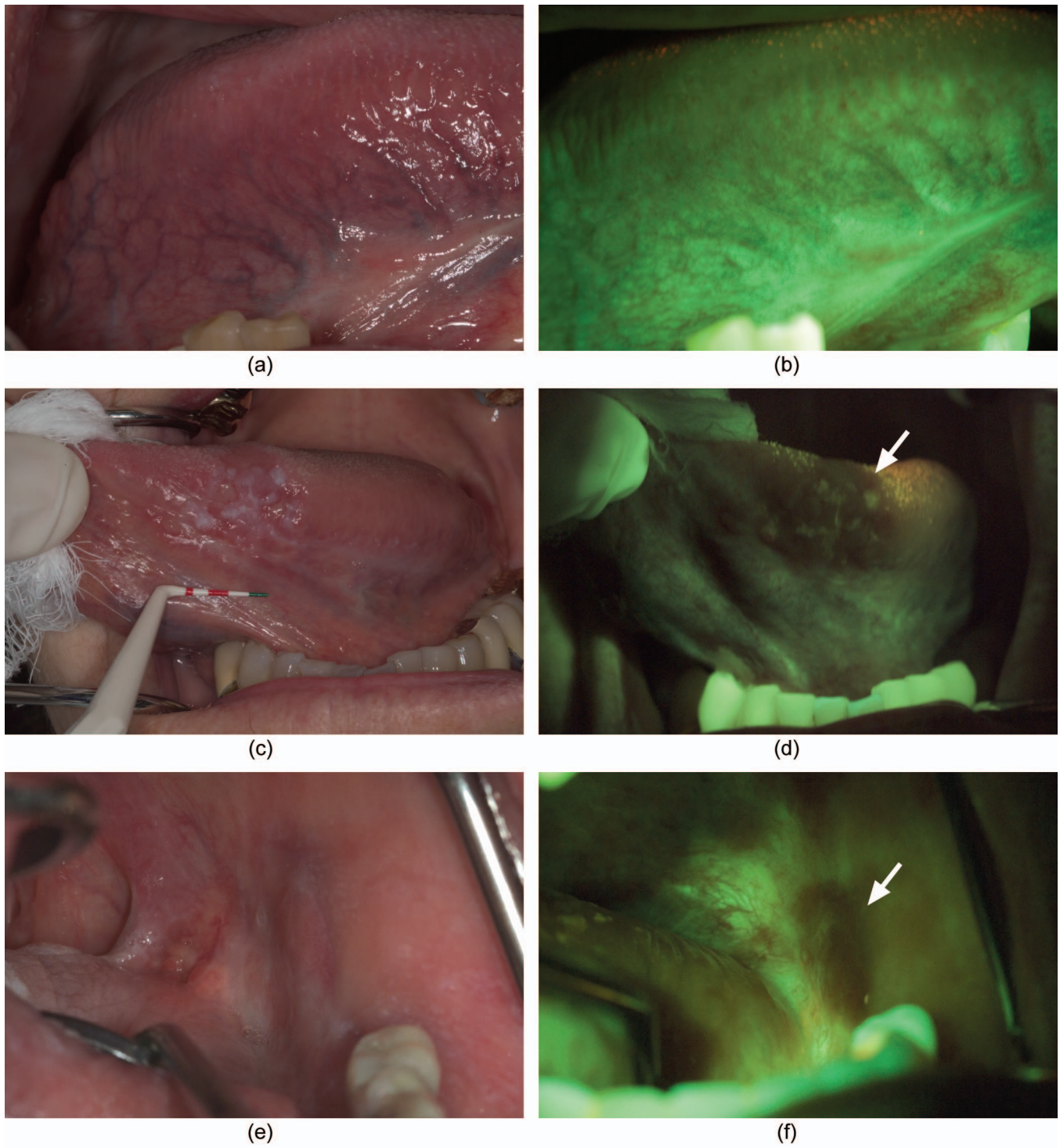


**Fig. 3** Photographs of three cases. White-light images are presented on the left and fluorescence images on the right. The top row illustrates normal mucosa of the ventral tongue—this healthy tissue has a pale-green fluorescence. The middle row shows the ventral tongue of a patient with an OPL, which when biopsied was confirmed to be a severe dysplasia. Arrow in panel (d) indicates region of biopsy and FVL. Bottom row shows a clinically occult lesion under white light, panel (e), and a corresponding dark patch (indicated with arrow) with FVL under direct FV.

**Table 1** Correlation of direct FV results with lesion histopathology.

	Normal	Severe Dysplasia and CIS	Invasive SCC	<i>P</i> value <sup>a</sup>
Number of lesions	6	11	33	
FVR	6 (100%)	1 (9%)	0 (0%)	<0.0001
FVL	0 (%)	10 (91%)	33 (100%)	

<sup>a</sup>2 × 2 chi squared of normal versus abnormal pathology (severe dysplasia, CIS, and SCC) and direct FV status.

As shown in Table 1, of the 50 biopsy samples, 7 samples were FVR, and 43 samples were FVL. None of the 6 samples with a histological diagnosis of normal showed loss of FV, whereas 91% of high-grade preinvasive lesions (severe dysplasia and CIS) and 100% of invasive SCC showed loss of FV ( $P < 0.0001$ , Fig. 3). Using histology as the gold standard, the device achieved a sensitivity of 98% and specificity of 100% when discriminating normal lesions from high-risk OPLs and invasive SCC.

#### 4 Discussion

These biopsy-confirmed preliminary results suggest that this direct FV device has potential as a simple, cost-effective screening device for the early detection of oral premalignant lesions. As in other sites, oral tissue autofluorescence characteristics seem to include information associated with the histopathological organization of the epithelial tissue.

Significant progress has been made in understanding the mechanisms responsible for endogenous fluorescence from epithelial tissues and how this fluorescence changes with dysplastic progression.<sup>26–29</sup> Fluorescence detected at the tissue surface is a function of tissue morphology and biochemistry. The intrinsic fluorescence, due to naturally occurring fluorophores in the epithelium and stroma, is modified by local tissue morphology through absorption and scattering, first during excitation, and then during emission. In general, the absorption and scattering modify the intensity and spectral distribution of the detected fluorescence.

The fluorophores of interest here are those that excite in the blue and have properties that have been spectroscopically correlated with dysplastic progression. The reduced form of nicotinamide adenine dinucleotide (NADH) and the oxidized form of flavin adenine dinucleotide (FAD) are important fluorophores that are good indicators of cellular metabolism. It has been shown that fluorescence intensity due to NADH increases with dysplastic progression and that of FAD decreases.<sup>27,29</sup> Maximum NADH fluorescence occurs at 340-nm excitation and 450-nm emission (but NADH is not interrogated by the device described here), while that of FAD occurs at 450-nm excitation and 515-nm emission<sup>26</sup> and is interrogated by this device. Another source of autofluorescence originates in the submucosa from collagen cross-links and has been shown to decrease in the immediate vicinity of dysplasia.<sup>27</sup> This loss of fluorescence is generally attributed to changes in collagen biochemistry, possibly due to the breakdown of the extracellular matrix by dysplastic cells. One hypothesis is that matrix metalloproteinases (MMP) expression in host stromal cells and the consequent remodeling of the

extracellular matrix is induced by altered signaling from dysplastic epithelial cells.<sup>30,31</sup> The excitation and emission bands of collagen cross-links are much broader than those of NADH/FAD, probably due to the contribution of several different fluorophores to the overall spectrum. Collagen yields maximum fluorescence at 340-nm excitation (420-nm emission) and has significant fluorescence when excited between 410 and 470 nm. In this region, the emission maximum continuously shifts to the red from 475 nm at 410-nm excitation to ~540 nm at 470-nm excitation.<sup>32</sup> Collagen-generated signals likely make up a significant fraction of the autofluorescent light detected by this device.

Tissue morphology affects fluorescence via absorption and scattering of the excitation and emission signals. The morphological changes that accompany dysplastic progression also affect the absorption and scattering properties of the tissue, which in turn modifies the fluorescence. It has been shown that nuclear changes observed during dysplastic progression increase nuclear scattering in cultured cells<sup>33</sup> and cells from cervical biopsies measured *ex vivo*.<sup>34</sup> The increased microvascularization that accompanies carcinogenesis leads to increased light absorption at 420 nm due to a higher hemoglobin concentration.

Based on the present knowledge of the origins of fluorescence and its change with dysplastic progression, we believe that the loss of fluorescence associated with dysplastic progression in the current device, which employs excitation from 400 to 460 nm and emission >475 nm, is primarily due to breakdown of the collagen matrix and increased hemoglobin absorption. Secondary to these effects is increased scattering in the epithelium, epithelial thickening, and a decrease in FAD concentration.

Fortuitously, studies by other researchers have identified excitation and emission wavelengths very similar to those employed by the present device for the optimal discrimination of normal and abnormal tissue. In a fluorescence spectroscopy study of 343 oral sites from 76 patients, Heintzelman et al.,<sup>10</sup> determined that the optimal excitation wavelengths for detecting neoplasia were 350, 380, and 400 nm. In a subsequent paper, Utzinger et al. point out that the response of the human eye should be considered when choosing the excitation and emission bands.<sup>22</sup> Using the Heintzelman et al. data, the authors show that abnormal tissue is optimally perceived with excitation between 420 and 440 nm. They also suggest observing fluorescence emission in a 50-nm band centered at 515 nm to increase the perceivable contrast between normal and abnormal tissue. Svistun et al.<sup>21</sup> extended the previous work by photographing freshly respected oral tissue using the

excitation wavelengths supported by the previous two studies (350, 380, 400, and 440 nm) and an emission band between 500 and 560 nm. The best sensitivity and specificity were achieved at 400- and 440-nm (our device uses 440- to 460-nm) excitation and the least favorable results were obtained at 340 nm.

Note that previously, the complex devices that record tissue fluorescence required very sensitive cameras or special tripods to reduce motion artifacts during long exposures. CCD-based instruments often incorporated postprocessing hardware to pseudocolor the final image for display. While this improves the contrast between normal and abnormal tissue it increases the cost and complexity of the instrument, making it unacceptable for large-scale deployment for a screening application. Note that all of the devices with similar performance discussed in the De Veld review employed only indirect visualization for the classification of lesions. In contrast, our simple, robust device facilitates the visualization of oral cavity fluorescence directly by a human observer. In addition to its application in precancer screening, this simple device could also be employed for biopsy guidance and margin delineation during surgical resection.

## 5 Summary

A simple field-of-view device for the direct visualization of tissue fluorescence was presented. The handheld unit was designed for the detection of high-risk oral premalignant lesions and SCC; however, the same instrument is easily translated to other organ sites. The design employs coaxial excitation and emission to reduce inter- and intraobserver variability.

Using histology as the gold standard for 50 sites, the device achieved a sensitivity of 98% and specificity of 100% when discriminating normal from high-risk OPLs and invasive SCC. It is envisioned that such a device would be used as an adjunct to conventional white-light screening to increase the sensitivity of white-light screen alone but not reduce the specificity.

## Acknowledgments

This work was supported by Grants R01-DE13124 and R01-DE17013 from the National Institute of Dental and Craniofacial Research (NIDCR). CP is supported by a Clinician Scientist Award from the Canadian Institute of Cancer Research.

## References

1. J. Ferlay, F. Bray, P. Pisani, and D. M. Parkin, "GLOBOCAN 2002: cancer incidence, mortality and prevalence worldwide," *IARC CancerBase No. 5*, version 2.0 ed., IARC Press, Lyon (2004).
2. American Cancer Society, "Cancer facts and figures 2005," Publication No. 5008.05, American Cancer Society, Atlanta, GA (2005).
3. A. L. Carvalho, I. N. Nishimoto, J. A. Califano, and L. P. Kowalski, "Trends in incidence and prognosis for head and neck cancer in the United States: a site-specific analysis of the SEER database," *Int. J. Cancer* **114**, 806–816 (2005).
4. A. Gillenwater, R. Jacob, R. Ganeshappa, B. Kemp, A. K. El-Naggar, J. L. Palmer, G. Clayman, M. F. Mitchell, and R. Richards-Kortum, "Noninvasive diagnosis of oral neoplasia based on fluorescence spectroscopy and native tissue autofluorescence," *Arch. Otolaryngol. Head Neck Surg.* **124**, 1251–1258 (1998).
5. S. Lam, C. MacAulay, J. Hung, J. LeRiche, A. E. Profio, and B. Palcic, "Detection of dysplasia and carcinoma in situ with a lung imaging fluorescence endoscope device," *J. Thorac. Cardiovasc. Surg.* **105**, 1035–1040 (1993).
6. N. Ramanujam, M. F. Mitchell, A. Mahadevan, S. Warren, S. Thomsen, E. Silva, and R. Richards-Kortum, "In-vivo diagnosis of cervical intraepithelial neoplasia using 337-nm-excited laser-induced fluorescence," *Proc. Natl. Acad. Sci. U.S.A.* **91**, 10193–10197 (1994).
7. H. Zeng, D. I. McLean, C. MacAulay, and H. Lui, "Autofluorescence properties of skin and applications in dermatology," *Proc. SPIE* **4224**, 366–373 (2000).
8. S. P. Schantz, V. Kolli, H. E. Savage, G. P. Yu, J. P. Shah, D. E. Harris, A. Katz, R. R. Alfano, and A. G. Huvos, "In vivo native cellular fluorescence and histological characteristics of head and neck cancer," *Clin. Cancer Res.* **4**, 1177–1182 (1998).
9. C. S. Betz, M. Mehlmann, K. Rick, H. Stepp, G. Grevers, R. Baumgartner, and A. Leunig, "Autofluorescence imaging and spectroscopy of normal and malignant mucosa in patients with head and neck cancer," *Lasers Surg. Med.* **25**, 323–334 (1999).
10. D. L. Heintzelman, U. Utzinger, H. Fuchs, A. Zuluaga, K. Gossage, A. M. Gillenwater, R. Jacob, B. Kemp, and R. R. Richards-Kortum, "Optimal excitation wavelengths for in vivo detection of oral neoplasia using fluorescence spectroscopy," *Photochem. Photobiol.* **72**, 103–113 (2000).
11. M. G. Muller, T. A. Valdez, I. Georgakoudi, V. Backman, C. Fuentes, S. Kabani, N. Laver, Z. M. Wang, C. W. Boone, R. R. Dasari, S. M. Shapshay, and M. S. Feld, "Spectroscopic detection and evaluation of morphologic and biochemical changes in early human oral carcinoma," *Cancer* **97**, 1681–1692 (2003).
12. D. R. Ingrams, J. K. Dhingra, K. Roy, D. F. Perrault, I. D. Bottrill, S. Kabani, E. E. Rebeiz, M. M. Pankratov, S. M. Shapshay, R. Manoharan, I. Itzkan, and M. S. Feld, "Autofluorescence characteristics of oral mucosa," *Head Neck* **19**, 27–32 (1997).
13. M. Inaguma and K. Hashimoto, "Porphyrin-like fluorescence in oral cancer—in vivo fluorescence spectral characterization of lesions by use of a near-ultraviolet excited autofluorescence diagnosis system and separation of fluorescent extracts by capillary electrophoresis," *Cancer* **86**, 2201–2211 (1999).
14. B. Kulapaditharom and V. Boonkitticharoen, "Performance characteristics of fluorescence endoscope in detection of head and neck cancers," *Ann. Otol. Rhinol. Laryngol.* **110**, 45–52 (2001).
15. D. C. G. De Veld, M. J. H. Witjes, H. J. C. M. Sterenberg, and J. L. N. Roodenburg, "The status of in vivo autofluorescence spectroscopy and imaging for oral oncology," *Oral Oncol.* **41**, 117–131 (2005).
16. K. Onizawa, H. Saginoya, Y. Furuya, H. Yoshida, and H. Fukuda, "Usefulness of fluorescence photography for diagnosis of oral cancer," *Int. J. Oral Maxillofac. Surg.* **28**, 206–210 (1999).
17. K. Onizawa, H. Saginoya, Y. Furuya, and H. Yoshida, "Fluorescence photography as a diagnostic method for oral cancer," *Cancer Lett.* **108**, 61–66 (1996).
18. C. S. Betz, H. Stepp, P. Janda, S. Arbogast, G. Grevers, R. Baumgartner, and A. Leunig, "A comparative study of normal inspection, autofluorescence and 5-ALA-induced PPIX fluorescence for oral cancer diagnosis," *Int. J. Cancer* **97**, 245–252 (2002).
19. R. Paczona, S. Temam, F. Janot, P. Marandas, and B. Lubinski, "Autofluorescence videoendoscopy for photodiagnosis of head and neck squamous cell carcinoma," *Eur. Arch. Otorhinolaryngol.* **260**, 544–548 (2003).
20. S. Lam, C. MacAulay, J. Hung, J. Leriche, A. E. Profio, and B. Palcic, "Detection of dysplasia and carcinoma in situ with a lung imaging fluorescence endoscope device," *J. Thorac. Cardiovasc. Surg.* **105**, 1035–1040 (1993).
21. E. Svistun, R. Alizadeh-Naderi, A. El-Naggar, R. Jacob, A. Gillenwater, and R. Richards-Kortum, "Vision enhancement system for detection of oral cavity neoplasia based on autofluorescence," *Head Neck* **26**, 205–215 (2004).
22. U. Utzinger, M. Bueeler, S. Oh, D. L. Heintzelman, E. S. Svistun, M. Abd-El-Barr, A. Gillenwater, and R. Richards-Kortum, "Optimal visual perception and detection of oral cavity neoplasia," *IEEE Trans. Biomed. Eng.* **50**, 396–399 (2003).
23. H. Lui, S. Said, L. Warshawski, D. Zloty, D. McLean, C. MacAulay, and H. Zeng, "Fluorescence visualization with blue light more accurately estimates the histopathologic margins of basal cell carcinoma as compared to clinical examination alone (abstract only)," 2001 SPIE/OSA European Conferences on Biomedical Optics, Munich, Germany, 2001.
24. H. Lui, S. Said, L. Warshawski, D. Zloty, D. McLean, C. MacAulay, and H. Zeng, "Fluorescence visualization with blue light more accurately estimates the histopathologic margins of basal cell carcinoma

- as compared to clinical examination alone (abstract only),” presented at IPA 8th World Congress of Photodynamic Medicine, Vancouver, BC Canada, 2001.
25. L. Zhang, M. Williams, C. F. Poh, D. Laronde, J. B. Epstein, S. Durham, H. Nakamura, K. Berean, A. Hovan, N. D. Le, G. Hislop, R. Priddy, J. Hay, W. L. Lam, and M. P. Rosin, “Toluidine blue staining identifies high-risk primary oral premalignant lesions with poor outcome,” *Cancer Res.* **65**, 8017–8021 (2005).
  26. R. Richards-Kortum and E. Sevick-Muraca, “Quantitative optical spectroscopy for tissue diagnosis,” *Annu. Rev. Phys. Chem.* **47**, 555–606 (1996).
  27. R. Drezek, C. Brookner, I. Pavlova, I. Boiko, A. Malpica, R. Lotan, M. Follen, and R. Richards-Kortum, “Autofluorescence microscopy of fresh cervical-tissue sections reveals alterations in tissue biochemistry with dysplasia,” *Photochem. Photobiol.* **73**, 636–641 (2001).
  28. R. Drezek, K. Sokolov, U. Utzinger, I. Boiko, A. Malpica, M. Follen, and R. Richards-Kortum, “Understanding the contributions of NADH and collagen to cervical tissue fluorescence spectra: modeling, measurements, and implications,” *J. Biomed. Opt.* **6**, 385–396 (2001).
  29. I. Pavlova, K. Sokolov, R. Drezek, A. Malpica, M. Follen, and R. Richards-Kortum, “Microanatomical and biochemical origins of normal and precancerous cervical autofluorescence using laser-scanning fluorescence confocal microscopy,” *Photochem. Photobiol.* **77**, 550–555 (2003).
  30. G. T. Thomas, M. P. Lewis, and P. M. Speight, “Matrix metalloproteinases and oral cancer,” *Oral Oncol.* **35**, 227–233 (1999).
  31. K. J. Heppner, L. M. Matrisian, R. A. Jensen, and W. H. Rodgers, “Expression of most matrix metalloproteinase family members in breast cancer represents a tumor-induced host response,” *Am. J. Pathol.* **149**, 273–282 (1996).
  32. K. Sokolov, J. Galvan, A. Myakov, A. Lacy, R. Lotan, and R. Richards-Kortum, “Realistic three-dimensional epithelial tissue phantoms for biomedical optics,” *J. Biomed. Opt.* **7**, 148–156 (2002).
  33. J. R. Mourant, M. Canpolat, C. Brocker, O. Esponda-Ramos, T. M. Johnson, A. Matanock, K. Stetter, and J. P. Freyer, “Light scattering from cells: the contribution of the nucleus and the effects of proliferative status,” *J. Biomed. Opt.* **5**, 131–137 (2000).
  34. T. Collier, D. Arifler, A. Malpica, M. Follen, and R. Richards-Kortum, “Determination of epithelial tissue scattering coefficient using confocal microscopy,” *IEEE J. Sel. Top. Quantum Electron.* **9**, 307–313 (2003).